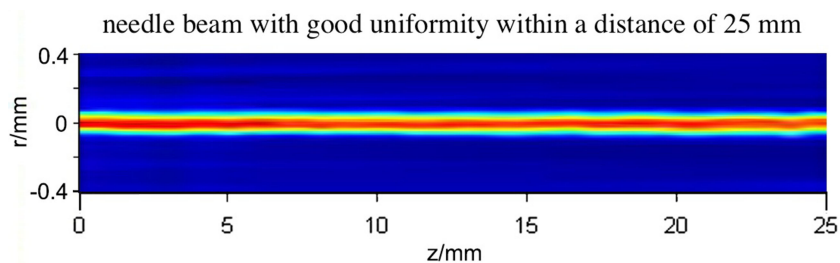


Needle Beam Generated by a Laser Beam Passing Through a Scattering Medium

Volume 10, Number 5, September 2018


Ziyang Chen
Xiansheng Hu
Xuanxuan Ji
Jixiong Pu



DOI: 10.1109/JPHOT.2018.2871216

1943-0655 © 2018 IEEE

Needle Beam Generated by a Laser Beam Passing Through a Scattering Medium

Ziyang Chen , Xiansheng Hu, Xuanxuan Ji, and Jixiong Pu 

College of Information Science and Engineering, Fujian Provincial Key Laboratory of Light Propagation and Transformation, Huaqiao University, Xiamen 361021, China

DOI:10.1109/JPHOT.2018.2871216

1943-0655 © 2018 IEEE. Translations and content mining are permitted for academic research only.

Personal use is also permitted, but republication/redistribution requires IEEE permission.

See http://www.ieee.org/publications_standards/publications/rights/index.html for more information.

Manuscript received August 13, 2018; revised September 4, 2018; accepted September 16, 2018. Date of publication September 19, 2018; date of current version October 3, 2018. This work was supported in part by the National Natural Science Foundation of China under Grants 11674111, 61575070, 61505059, and 11750110426, in part by the Fujian Province Science Funds for Distinguished Young Scholar under Grant 2018J06017, and in part by the Natural Science Foundation of Fujian Province under Grant 2017J01003. Corresponding author: Jixiong Pu (e-mail: jixiong@hqu.edu.cn).

Abstract: The propagation of coherent light through an inhomogeneous medium generates a speckle pattern caused by the complex interference of randomly scattered waves. The speckle pattern does not resemble the incident beam profile. However, the spatially random pattern can be reshaped into a bright focal spot by wavefront shaping. And, in general, the focused intensity is of maximum just at the focal plane, and the focused intensity of the shaped focal beam decreases sharply with incremental distance from the focal plane. In this paper, we report the experimental generation of a needle beam as the laser beam passes through a scattering medium. The intensity and beam size of the needle beam remain nearly intact within the distance of 25 mm, which indicates that the focal pattern has a uniform property.

Index Terms: Speckle, optical field modulation.

1. Introduction

The intensity modulations of focal patterns have become increasingly interesting due to their potential in laser processing and particle trapping [1], [2]. For example, the subwavelength needle pattern was demonstrated by using a binary-phase optical element in a high numerical aperture focusing system [3]. However, specifying the modulation of the intensity pattern in the presence of a scattering medium is a challenge. The propagation of laser beams through an optically scattering medium will result in the random scattering and distortion of the propagating wavefront. Such distortions delimit the effective focusing of light and degrading image quality. Random wave scattering and its complex interference produce well-known “speckle” interference patterns. Speckles are assumed to pose fundamental limitations on the resolution of optical methods. Ongoing efforts in recent years have focused on correcting the spatial distortions of waves by using wavefront-shaping and other techniques. In 2007, Vellekoop and Mosk demonstrated the effective focusing of light through a random-scattering medium [4]. Since this pioneering work, considerable research has been conducted on related topics [5]–[23]. Although light scatters in a complex and unknown manner, the scattering process is deterministic and can be tailored to refocus the beam in a desired fashion. Wavefront shaping has also been introduced in the modulation of random speckle field properties. Light can be focused on a tiny spot, such as those 10 times smaller than the usual diffraction limit, by

using scattering behind a lens [5]. This technique has led to the development of an imaging system with a resolution higher than 100 nm in visible wavelengths [6]. In addition, random speckles can be shaped into the desired focal patterns [7], [8]. The modulation of random speckle fields into desired patterns has a wide range of application in numerous fields, such as particle trapping, imaging, and microscopy [15]–[23].

A spatial light modulator (SLM) impresses a phase modulation on a laser beam, and the resulting field can be converted into the desired distribution by scattering through a diffuser. In a sense, if the SLM pre-compensates the distortion introduced by the diffuser, then the reconstruction of the input beam can be managed. However, although the focusing of laser beams through a scattering medium has been demonstrated, most studies have centered on shaping the random scattered speckle fields as bright focal spots on focal planes. The focused intensity can be maximized only at the focal plane. With the increment of the distance away from the focal plane, the focused intensity decreases. This characteristic may hamper the applicability of this technique in certain fields, such as particle trapping and acceleration. Some studies have been focused on the generation of a non-diffraction beam as a laser beam passing through the scattering medium. Ring-shaped spatial filters have been introduced in these studies, but this scheme can lessen the efficiency of incident light [24], [25]. Here, we report a novel approach to synthesize a needle beam with distance of 25 mm. The quality of the intensity pattern of this super-long structure remains nearly intact, and the focal pattern has shown good uniform properties within this range.

2. Theoretical Analysis

When light propagates through a scattering medium, the directions of wave vectors are scrambled by random scattering into microscopic particles and other inhomogeneities. If the incident light is divided into N segments, then the transmitted field at the target becomes the combination of the fields coming from these N segments [4], namely,

$$E_m = \sum_{n=1}^N t_{mn} A_n \exp(i\phi_n), \quad (1)$$

where A_n and ϕ_n are the amplitude and phase of a segment, respectively, and t_{mn} represents the element of the transmission matrix that describes the scattering of the medium and the propagation of the optical system. In principle, if all these segments interfere constructively at a target, then a bright focal spot can be generated. This generation can be achieved using a phase-only SLM to shape the wavefront of the incident light. The SLM is divided into N segments, and an algorithm is introduced to obtain the optimal shaping phase of each segment. After the modulation, a highly enhanced focal spot can be achieved. The enhancement is defined as [4]

$$\eta = \frac{I_{\text{obj}}}{I_{\text{initial}}}, \quad (2)$$

where I_{obj} is the intensity of the focal spot after optimization and I_{initial} is the average light intensity of the entire speckle field before the incident wave has been optimized.

3. Experimental Result and Discussion

Figure 1 shows the experimental setup of the wavefront-shaping technique. The expanded light beam from the He-Ne laser with a wavelength of 632.8 nm is reflected by an SLM at the frame rate of 60 Hz (Holoeye Pluto), i.e., the configuration used to modulate the phase of incident-coherent light. The SLM strongly depends on polarization, i.e., only the component of the incident electric field parallel to the liquid crystal (LC) director, representing the direction from which the LC molecules are aligned, can be purely phase modulated while the perpendicular component remains intact. Subsequently, a polarizer is inserted in front of the SLM. The light is focused by a high numerical

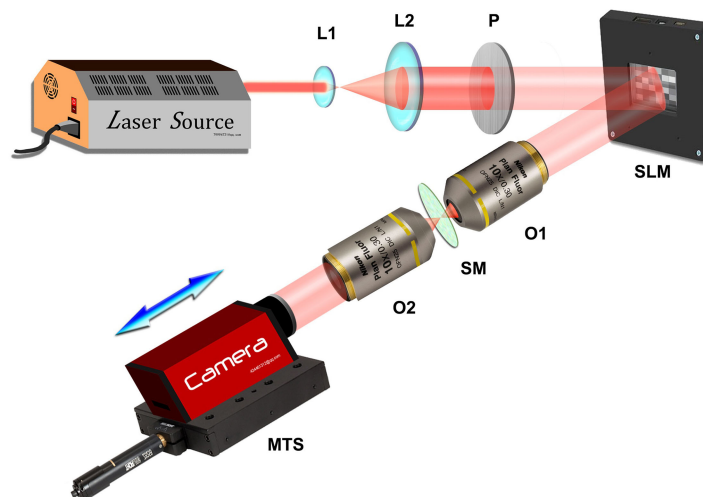


Fig. 1. Experimental setup. L1 and L2 are two lenses with focal lengths of 50 and 150 mm, respectively; P is a polarizer; SLM is a spatial light modulator; O1 and O2 are objectives with a numerical aperture of 0.3; SM is a scattering medium; and MTS is a motorized translation stage.

aperture objective, and the scattering medium (DG10-600, Thorlabs) is inserted near the objective focus. Another high numerical aperture objective is introduced to collect the scattering light. A charge-coupled device (CCD) camera (AVT PIKE, F421B) is used to monitor target intensity and provide feedback for the algorithm. On the basis of the feedback, the algorithm continues to calculate a proper phase map for the SLM until the desired result is achieved.

In the experiment, we built a genetic algorithm (GA) to modulate the phase of incident light. The GA is an extensively used iterative algorithm and has strong anti-disturbance capability [26]. The concrete steps are as follows. The randomly generated phase masks are initially loaded into the SLM one by one. Then, a series of related intensity values of the measurable target is taken as the adaptive values of the phase masks. Two phase masks, which are likely to be designated with high adaptive values, are selected as parents for new offspring generation. The randomly selected segments of the offspring are inherited from the corresponding phases of one of the phase masks while the remaining segments are inherited from the other mask. This new mask is then mutated by randomly changing the phase of the segment portions. A specific number of new phase masks generated by this suit replace the masks with the lowest adaptive values from the previous generation. Finally, the new generation is ranked on the basis of parent generation and measured adaptive values. This process continuously runs until the iteration reaches a certain number.

A random speckle pattern is generated when a coherent light transmits through a scattering medium (Fig. 2(a)). This unpredictable speckle pattern can be modulated as the desired focal spot by introducing an appropriate phase map on the incident light. An SLM divided into 30×30 segments is used to modulate the phase of incident light by adopting the desired phase map. In Fig. 2(b), we present the focal spot with intensity enhancement of 19.74 after phase modulation. Subsequently, we identify the focal spot on the focal plane. In most studies, researchers have paid attention to the transversal intensity distribution only at the focus. However, the distribution of intensity along the longitudinal direction is unclear. Nonetheless, the entire field distribution near the focal plane is an important consideration. We therefore assign a motorized translation stage by which the CCD is repositioned to record the 3D intensities near the focus. In Fig. 2(c), we present the 3D intensity distribution near the focus. In this case, the maximum focal intensity at the focus (Fig. 2(b)) is achieved after wavefront shaping. Moreover, as shown in Fig. 2(c), the maximum focal intensity is at $z = 10$ mm. The focused intensity decreases with the increment of the distance away

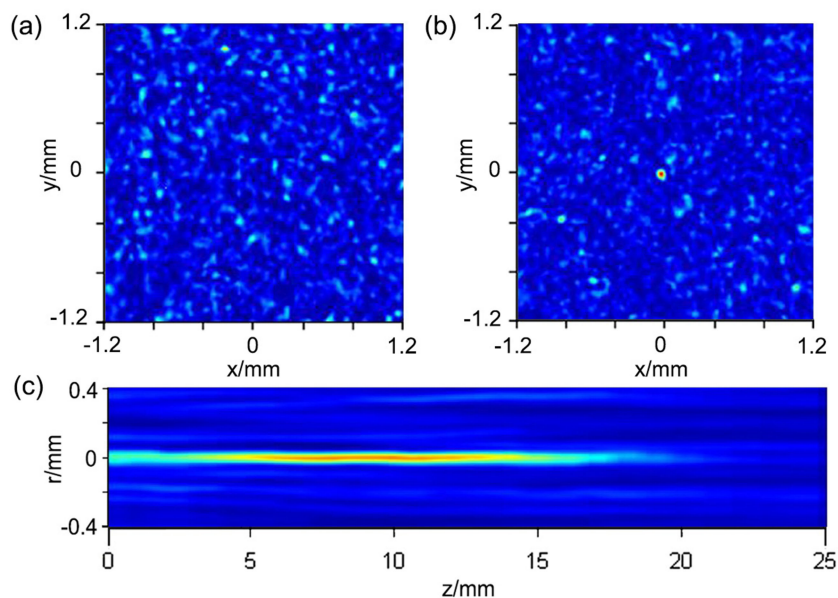


Fig. 2. (a) Random speckle pattern formed by a coherent laser through a scattering medium. (b) Bright focal spot generated by wavefront shaping. (c) Intensity distribution near the focus generated by wavefront shaping.

from the focus. The full width at half maximum (FWHM) along the longitudinal direction of the focal spot is estimated to be 12.6 mm.

As demonstrated above, the random speckle pattern can be modulated as a bright focal spot by feedback wavefront shaping, and the 3D intensity distribution behaves similar to that of a focused light beam, which is uncontrolled. Can we modulate intensity distribution both at the focus and along the longitudinal direction (i.e., 3D intensity distribution near the focus)? A feedback is needed to generate the focal spot at the focus for the light beam passing through the scattering medium. Similarly, a scheme for intensity distribution along the focal line must be introduced as feedback to control the 3D intensity distribution and modulate this distribution near the focus. A movable CCD, which can record 3D intensity distribution (i.e., introduced as the feedback), is then used. In this case, we can achieve the desired 3D field distribution near the focus. We will experimentally demonstrate that a needle beam can be produced by modulating the phase of the incident light beam.

The 3D intensity distribution needs to be monitored and used as the algorithm feedback to produce a needle beam after passing through the scattering medium. In the experiment, the CCD affixed on the motorized translation stage (PT1/M-Z8, Thorlabs) is movable. The scanning distance is 25 mm, and the intensity distributions at the four planes ($z = 0, 8, 16,$ and 24 mm) are recorded as the algorithm feedback. On the one hand, the computing time of the algorithm increases when numerous planes are recorded. On the other hand, the uniform properties of the needle beam are difficult to determine if few planes are recorded.

In general, when a focal spot is generated, only a single intensity result is used as the algorithm feedback, and the optimal result is a highly enhanced focus. In the present work, the intensity distributions at the four positions along the focal line are adopted as feedback to generate a super-long focal line. Subsequently, the optimal result corresponding to the selected positions requires not only intensities that are highly enhanced but also intensities with uniform properties. Therefore, the cost function of the algorithm should focus on maximizing the intensity of the focal spots while restricting large differences in intensity values. The cost function is defined as the summation of all focused intensities minus a coefficient multiplied by the standard deviation of the intensities of the

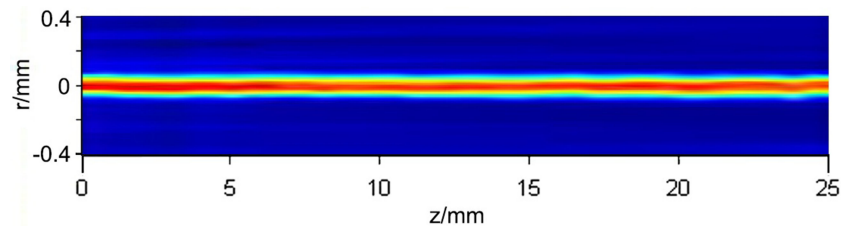


Fig. 3. Generated needle beam formed by a laser beam that passes through a scattering medium.

focused spots, which can be expressed as [27]

$$C = \sum_{m=1}^4 I_m - M \cdot \sigma(I). \quad (3)$$

The above equation indicates that the cost function covers the enhancement and uniformity of the intensity distribution at the four positions. The balance between enhancement and uniformity can be controlled by the coefficient M . Enhancement is more important with low M values, whereas uniformity is more important with high M valued. The objective of this study is to balance high enhancement with good uniformity.

The movable CCD traces the transverse intensity distribution along the focal line by using a proper cost function. The intensity distribution along the focal line can be controlled for laser beams that pass through a scattering medium. We then use a movable CCD with a scanning length of 25 mm to record the intensity distributions at the four positions of 0, 8, 16, and 24 mm. A focal pattern with the desired distribution can be generated by using the intensities at the four positions (i.e., GA feedback) and by introducing the feedback wavefront-shaping technique to modulate the phase of the incident beam. After the optimization of the wavefront of the incident light beam is achieved using the SLM with 30×30 segments, the needle beam is obtained (Fig. 3). The intensity distribution of the generated needle beam is uniform within a distance of 25 mm. In scanning process of the 3D distribution of the needle beam, the objective (O2) is fixed. Therefore, the needle beam focusing is not exactly behind a scattering layer, but behind the scattering medium coupled with an objective lens. The focus is in fact laying at the camera planes, not exactly right at the exit of the scattering layer.

Then, we measure the transversal intensity distribution along the focal line. The averaged transversal FWHM size of the focal beams is approximately $118.4 \mu\text{m}$ within a distance of 25 mm. The maximal and minimal enhancements of the intensity distributions along the focal line are 22.25 and 19.54, respectively. The standard deviation of the enhancements is calculated to be 0.468, which indicates that the intensity magnitude along the longitudinal axis has good uniformity. In the generation of the focal line, the intensity distribution of the pixel area (3×3) of the focal plane is used as the target, and the focal patterns at several distances are adopted as the feedback.

The evolution of the cost function of the needle beam generation is shown in Fig. 4. Before modulation, random speckle patterns are generated, and the intensities in the four monitor planes are low and not uniform. The cost function in Eq. (3) includes the summation and standard deviation of the intensity magnitude of the target in the four planes. The high intensity and good uniformity of the four planes results in an incremental cost function. After the algorithm is run, the intensities of the targets increase gradually, and the intensities at the four planes become highly uniform. Therefore, the cost function improves with algorithm iteration.

Fig. 5 shows the intensity distributions at the four positions (2.5, 9.5, 16.5, and 23.5 mm) along the focal line. The focal intensity enhancements at the four distances are estimated to be 21.875, 19.792, 20.313, and 19.914. The beam width and intensity magnitude of the focal spots has remained nearly invariant within the distance of 25 mm, thereby showing good intensity uniformity.

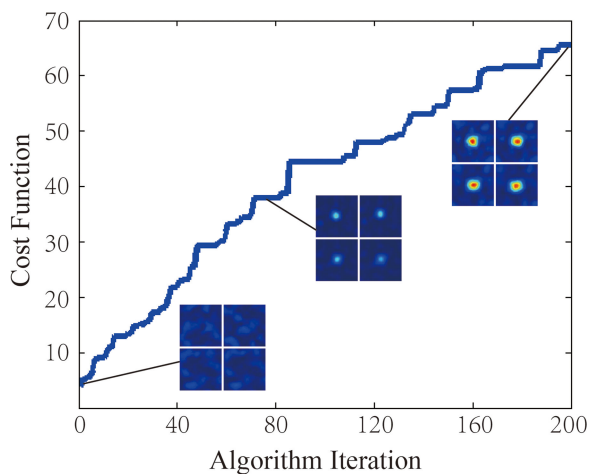


Fig. 4. Evolution of the cost function for needle beam generation.

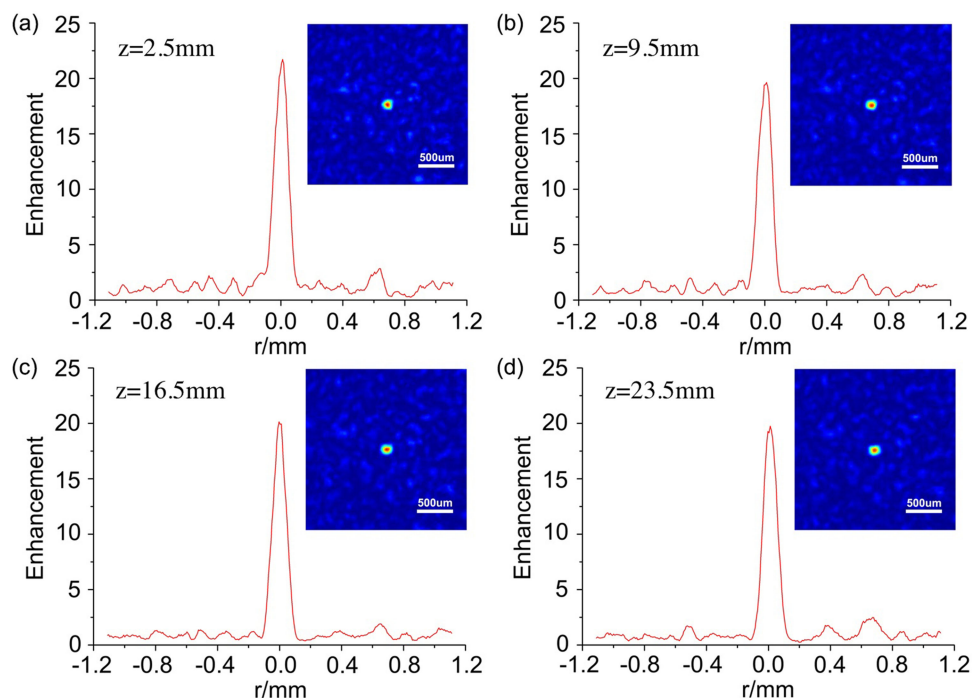


Fig. 5. Transversal intensity distribution along the focal line at the four positions of (a) 2.5 mm, (b) 9.5 mm, (c) 16.5 mm, and (d) 23.5 mm.

Although the needle beam in Fig. 4 shows good uniformity within the distance of 25 mm, this characteristic cannot be preserved outside this region. The beam decay of the needle beam after the distance of 25 mm is presented in Fig. 6. Intensity enhancement decreases as we move farther away the CCD. The result indicates that the uniformity characteristic of the intensity distribution can be attributed only to the region selected for the algorithm feedback. It can be found that the whole needle beam is constituted by a relatively steady center part (Fig. 3) and two progressively decreasing wings (Fig. 6). The central steady part stretches about 21 mm, and half width at half maximum of a wing is 32.49 mm (This result is calculated from Gaussian function which is fitted by

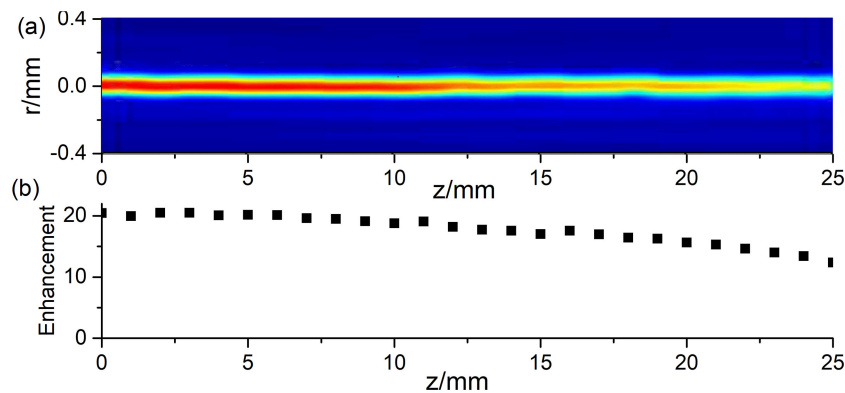


Fig. 6. (a) Beam decay after the range of the needle beam as recorded by the backward-moving CCD. (b) Evolution of intensity enhancement after the range of the needle beam.

data in Fig. 3 and Fig. 6). The total length of needle beam is approximately 86 mm, which is 6.8 times of the length (12.6 mm) generated by a single focal spot optimization shown in Fig. 2.

4. Conclusion

The speckle pattern formed by a laser beam through a scattering medium is modulated by using a super-long focal line. The 3D intensity distribution of the speckle pattern is monitored by a movable CCD and then used as the feedback of the wavefront-shaping algorithm. An intensity distribution with good uniformity within a distance of 25 mm is generated on the basis of the GA. The transversal size of the focal spot is approximately $118.4 \mu\text{m}$ and remains intact within this distance, which indicates that the focal pattern has uniform properties. The maximal and minimal enhancements of the focal spots are estimated to be 22.25 and 19.54, respectively, which imply that the focal spots have high intensity increments.

References

- [1] D. B. Phillips *et al.*, "Shape-induced force fields in optical trapping," *Nature Photon.* vol. 8, no. 5, pp. 400–405, 2014.
- [2] Q. Zhan, "Cylindrical vector beams: From mathematical concepts to applications," *Adv. Opt. Photon.*, vol. 1, no. 1, pp. 1–57, 2009.
- [3] H. Wang, L. Shi, B. Lukyanchuk, C. Sheppard, and C. T. Chong, "Creation of a needle of longitudinally polarized light in vacuum using binary optics," *Nature Photon.*, vol. 2, no. 8, pp. 501–505, 2008.
- [4] M. Vellekoop and A. P. Mosk, "Focusing coherent light through opaque strongly scattering media," *Opt. Lett.*, vol. 32, no. 16, pp. 2309–2311, 2007.
- [5] M. Vellekoop, A. Lagendijk, and A. P. Mosk, "Exploiting disorder for perfect focusing," *Nature Photon.*, vol. 4, no. 5, pp. 320–322, 2010.
- [6] E. G. van Putten, D. Akbulut, J. Bertolotti, W. L. Vos, A. Lagendijk, and A. P. Mosk, "Scattering lens resolves sub-100 nm structures with visible light," *Physical Rev. Lett.*, vol. 106, no. 19, 2011, Art. no. 193905.
- [7] D. B. Conkey and R. Piestun, "Color image projection through a strongly scattering wall," *Opt. Exp.*, vol. 20, no. 25, pp. 27312–27318, 2012.
- [8] L. Wan, Z. Chen, H. Huang, and J. Pu, "Focusing light into desired patterns through turbid media by feedback-based wavefront shaping," *Appl. Phys. B*, vol. 122, no. 7, p. 204, 2016.
- [9] Katz, E. Small, Y. Bromberg, and Y. Silberberg, "Focusing and compression of ultrashort pulses through scattering media," *Nature Photon.*, vol. 5, no. 6, pp. 372–377, 2011.
- [10] J. Aulbach, B. Gjonaj, P. M. Johnson, A. P. Mosk, and A. Lagendijk, "Control of light transmission through opaque scattering media in space and time," *Physical Rev. Lett.*, vol. 106, no. 10, 2011, Art. no. 103901.
- [11] H. P. Paudel, C. Stockbridge, J. Mertz, and T. Bifano, "Focusing polychromatic light through strongly scattering media," *Opt. Exp.*, vol. 21, no. 14, pp. 17299–17308, 2013.
- [12] E. Small, O. Katz, Y. F. Guan, and Y. Silberberg, "Spectral control of broadband light through random media by wavefront shaping," *Opt. Lett.*, vol. 37, no. 16, pp. 3429–3431, 2012.
- [13] Y. F. Guan, O. Katz, E. Small, J. Y. Zhou, and Y. Silberberg, "Polarization control of multiply scattered light through random media by wavefront shaping," *Opt. Lett.*, vol. 37, no. 22, pp. 4663–4665, 2012.

- [14] N. K. Soni, R. V. Ninu, and R. K. Singh, "Polarization modulation for imaging behind the scattering medium," *Opt. Lett.*, vol. 41, no. 5, pp. 906–909, 2016.
- [15] K. Dholakia and T. Cizmar, "Shaping the future of manipulation," *Nature Photon.*, vol. 5, no. 6, pp. 335–342, 2011.
- [16] S. Kang *et al.*, "Imaging deep within a scattering medium using collective accumulation of single-scattered waves," *Nature Photon.*, vol. 9, no. 4, pp. 253–258, 2015.
- [17] R. Horstmeyer *et al.*, "Guidestar-assisted wavefront-shaping methods for focusing light into biological tissue," *Nature Photon.*, vol. 9, no. 9, pp. 563–571, 2015.
- [18] R. K. Singh, A. M. Sharma, and B. Das, "Quantitative phase-contrast imaging through a scattering media," *Opt. Lett.*, vol. 39, no. 17, pp. 5054–5057, 2014.
- [19] C. Gohn-Kreuz and A. Rohrbach, "Light needles in scattering media using self-reconstructing beams and the STED principle," *Optica*, vol. 4, no. 9, pp. 1134–1142, 2017.
- [20] H. Yu, K. Lee, J. Park, and Y. Park, "Ultrahigh-definition dynamic 3D holographic display by active control of volume speckle fields," *Nature Photon.*, vol. 11, no. 3, pp. 186–188, 2017.
- [21] M. Liao, D. Lu, W. He, and X. Peng, "Optical cryptanalysis method using wavefront shaping," *IEEE Photon. J.*, vol. 9, no. 1, Feb. 2017, Art. no. 2200513.
- [22] Y. Zhou and X. Li, "Optimization of iterative algorithms for focusing light through scattering media," *IEEE Photon. J.*, vol. 9, no. 2, Apr. 2017, Art. no. 6100310.
- [23] D. D. Battista *et al.*, "Tailored light sheets through opaque cylindrical lenses," *Optica*, vol. 3, no. 11, pp. 1237–1240, 2016.
- [24] D. D. Battista, D. Ancora, M. Leonetti, and G. Zacharakis, "Tailoring non-diffractive beams from amorphous light speckles," *Appl. Phys. Lett.*, vol. 109, no. 12, 2016, Art. no. 121110.
- [25] A. Boniface, M. Mounaix, B. Blochet, R. Piestun, and S. Gigan. "Transmission-matrix-based point-spread-function engineering through a complex medium," *Optica*, vol. 4, no. 1, pp. 54–59, 2017.
- [26] D. B. Conkey, A. N. Brown, A. M. Caravaca-Aguirre, and R. Piestun, "Genetic algorithm optimization for focusing through turbid media in noisy environments," *Opt. Exp.*, vol. 20, no. 5, pp. 4840–4849, 2012.
- [27] D. B. Conkey and R. Piestun, "Color image projection through a strongly scattering wall," *Opt. Exp.*, vol. 20, no. 25, pp. 27312–27318, 2012.